ELSEVIER

Journal of Magnetism and Magnetic Materials 251 (2002) 100–108

journal of magnetism and magnetic materials

www.elsevier.com/locate/jmmm

Permeability measurements in cobalt ferrite and carbonyl iron powders and suspensions

J. de Vicente[a,*], G. Bossis[b], S. Lacis[c], M. Guyot[d]

[a] *Departamento de Física Aplicada, Facultad de Ciencias, Universidad de Granada, C/Fuentenueva s/n, 18071 Granada, Spain*
[b] *Laboratoire de Physique de la Matière Condensée, Université de Nice-Sophia Antipolis, Parc Valrose, 06108 Nice Cedex 2, France*
[c] *Department of Physics, University of Latvia, LV-1586 Riga, Latvia*
[d] *Laboratoire de Magnétisme et d'Optique, 45 Avenue des Etats-Unis, 78035 Versailles, France*

Received 16 April 2002; received in revised form 8 July 2002

Abstract

Magnetic permeability data of cobalt ferrite and carbonyl iron suspensions are discussed. Using an induction method, the relative differential permeability, $\mu_{r,dif}$, was measured as a function of the internal magnetic field for different volume fractions of the solid phase. In the case of cobalt ferrite suspensions, the $\mu_{r,dif} - H$ curve was obtained for a first increasing ramp of magnetic field (data series "1"), a decreasing ramp (data series "2"), and the second increasing one (data series "3"). Series "1" showed a maximum in the $\mu_{r,dif} - H$ trend that did not appear in series "2" and "3". Furthermore, the data in series "2" and "3" are always below those in series "1". The latter behavior could be ascribed to the presence of hysteresis, and in fact it was not observed in carbonyl iron suspensions, where hysteresis is absent. The presence of the maximum in permeability is common for both types of suspensions. It is found that it only disappears if the particle motions are restricted by dispersing them in a rigid (epoxy) matrix, or if the suspensions are previously structured by applying a magnetic field to a sample prepared in an elastomer matrix. We conclude that the maxima in $\mu_{r,dif} - H$ curves are associated to the motion or orientation of the dispersed particles during application of the first field ramp. The comparison with predictions of models allows to deduce some quantitative information on the structures formed by the particles.
© 2002 Elsevier Science B.V. All rights reserved.

Keywords: Cobalt ferrite spherical particles; Magnetorheological fluids; Magnetic permeability; Magnetic structures; Induction method

1. Introduction

It is well known that the physical properties of suspensions of magnetic particles and, in particular, their magnetorheological characteristics, are to a large extent governed by the magnetic behavior of the dispersed solid particles. It is hence essential to properly determine such behavior if we intend to design a magnetic suspension for whatever purpose or to explain its macroscopic properties from a microscopic approach.

If, as it is often the case, the starting solid material is already powdered, the determination of its bulk magnetic permeability from measurements

*Corresponding author. Tel.: +34-958-249099; fax: +34-958-243214.
E-mail address: jvicente@ugr.es (J. de Vicente).

0304-8853/02/$ - see front matter © 2002 Elsevier Science B.V. All rights reserved.
PII: S0304-8853(02)00484-5

performed on the powder is quite difficult. For this reason it is often preferred to determine the magnetic properties of the dispersed particles in situ, i.e., to directly measure the permeability of the already prepared suspension and, from this, to infer that of the particles using the proper model to relate these quantities.

In this work, we report data on the relative differential permeability, $\mu_{r,dif}$, of cobalt ferrite and carbonyl iron suspensions of different volume fractions, as a function of the applied magnetic field. We shall emphasize the role of the motion or orientation of the particles during the measurements, and we shall see how we can infer structural information from the permeability measurements.

2. Methods for measuring the magnetic properties

Two types of force-balance methods have been devised for determining the magnetization, or equivalently the susceptibility, of materials [1]. These are the analytical balance and the torsion balance. In our case, we will use a modified susceptibility balance. A sample is suspended at the end of a long non-magnetic rod in the presence of a gradient of magnetic field. The magnetic potential energy, W, of a material of volume V and magnetization M, subjected to a magnetic field H is [2]

$$W = -\mu_0 VM \cdot H. \tag{1}$$

Assuming that the gradient has only x-component, and that the only non-zero component is the x one

$$F_x = \mu_0 VM_x \frac{dH_x}{dx} = \mu_0 \chi VH_x \frac{dH_x}{dx}. \tag{2}$$

Here we observe that the force on the sample is proportional to its susceptibility. The limitations of the method are that it is only valid for small samples, and that a constant gradient of magnetic field is needed.

The induction methods are all dependent on Faraday's law of electromagnetic induction. Here one measures the magnetic flux, and determines the magnetic induction, B, from the knowledge of sample cross section normal to the field. The method used in this work is based on the Hartshorn bridge [3] which can be briefly described as follows. The sample is placed in the presence of a weak oscillating magnetic field, created by a primary coil, and the voltage difference (proportional to the sample's magnetization) between the ends of the measuring coil is measured. The latter consists in two compensated coils (secondary coils) connected in such a way that in the absence of sample the potential difference, ε, is zero. If the sample is present, the induced potential difference can be written:

$$\varepsilon = -\frac{B}{I}\chi V\tilde{H}\omega \cos \omega t, \tag{3}$$

where B is the magnetic induction, I is the current intensity, χ is the magnetic susceptibility, $\tilde{H}$ is the amplitude of the oscillating field and ω is its frequency. This method has the advantage that if a constant field is superimposed on the oscillating one, one can measure the susceptibility for different fields, and the whole magnetization curve of the sample can be obtained.

3. Experimental

3.1. Materials

The cobalt ferrite particles were synthesized as described in Ref. [4]. They were well spherical and monodisperse, with an average diameter of 850 ± 150 nm. Carbonyl iron powder was a commercial product from BASF (Germany), with an average diameter of about 1 μm, according to manufacturer's data.

3.2. Methods

The magnetometer used was a DSM-8 (France). The powder sample is introduced in a small Teflon container (1 mm^3 volume) which is fixed at the end of a brass rod. The sample is placed in the presence of an external magnetic field gradient perpendicular to the rod at 293.0 ± 0.2 K. A magneto-optic device detects the force by measuring the torsion angle of a wire. Then, a servo-controlled device

applies a compensation force that brings the sample rod back into its initial position.

The experimental setup for the induction method is shown schematically in Fig. 1a. It consists of a sinusoidal function generator (φ Francaise d'Instrumentation Generateur de Functions Digital FI 8115), an amplifier (Inkel MA-620), a digital amperimeter (HP 34401 A Multimeter), a Lock-in amplifier (MR 8, Princeton Applied Research model) and the so-called "system of coils" in which is in fact based. It consists of two electronic circuits coupled by means of two identical transformers (compensated), as well as an electromagnet (TBK elec. Paris, TE 90 AS). The first circuit is called primary circuit, and it consists of a pair of coils in series opposition. The purpose of these coils is to create the AC magnetic field (frequency 1200 Hz) that the sample will feel: in each of the coils there is a coil of the secondary circuit. One of the latter contains the sample. All the coils have 1000 turns and are as similar as possible. However, since they cannot be absolutely identical, a calibration procedure is needed, and for that reason the secondary circuit also includes two resistors (R_1, R_2), and a potentiometer (R_3) in addition to the coils (L_1, L_2), as shown schematically in Fig. 1b. The calibration is considered complete when the potential difference V_{CD} is zero when there is no sample in the system.

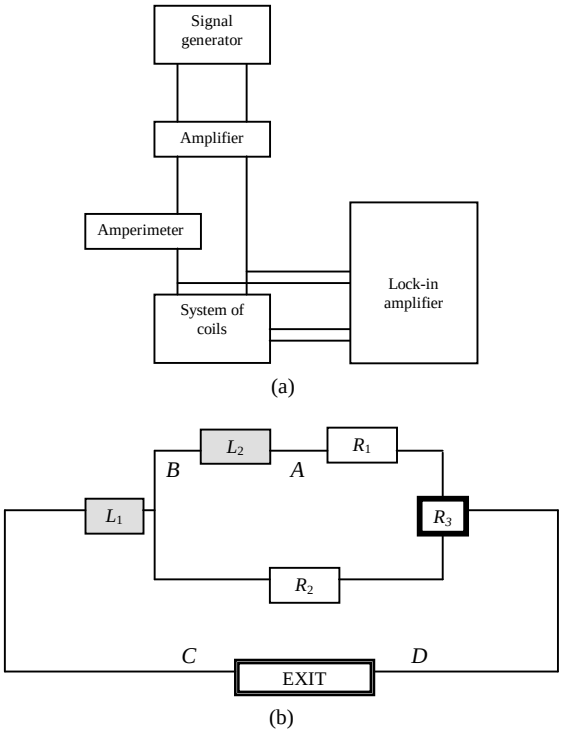

Fig. 1. (a) Schematics of the device for the measurement of the differential permeability in MR-suspensions. (b) Schematic representation of the secondary circuit.

The purpose of this device is to measure the differential susceptibility of the sample by means of the electric current that this material induces in a coil when placed inside. The word "differential" has its origin in the method used: we measure the slope of the magnetization curve. In order to do that we superimpose the oscillating magnetic field and a constant one, generated by the electromagnet.

Once the calibrations are performed, both of the secondary circuit and the electromagnet, we can assume that the former consists of two identical transformers. Then, the potential difference at the exit can be written (Fig. 1b):

$$V_{CD} = 4\pi 10^{-8} \omega MNs, \tag{4}$$

where V_{CD} is in volts, M (sample magnetization) in emu, s (cross section of the sample perpendicular to the external magnetic field) in cm^2, and N is the number of turns in the coils. It is important to remark that the amplitude of the probe AC field is always much lower than that of the constant one.

We performed measurements in stable ferrite suspensions (particle volume fraction: $\phi = 0.2$). The dispersion medium used in this work was always silicone oil (47V20 from Rhône-Poulenc, France) of density $0.95\,g\,cm^{-3}$ and viscosity 20 mPa s. With the purpose of minimizing the sedimentation we added a small amount of silica gel (Aerosil 300 from Degussa, USA) consisting of fine spherical particles of SiO_2, 7 nm in diameter. The Aerosil added in each suspension is 1.5% the mass of the suspension. The Aerosil particles form a 3D network where the ferrite particles are placed [5]. In all cases, we used cylindrical sample holders of cross section $0.077\,cm^2$ and average length 3.3 cm.

In the case of carbonyl iron suspensions, differential permeability was measured for volume

fractions ranging from about 12% to about 60% in two different dispersion media: silicone oil + Aerosil, and in a silicone elastomer matrix (RTV 851 and catalyst 11016, from Rhodosil, France).

4. Results and discussion

4.1. Magnetometry of cobalt ferrite particles

Fig. 2 shows the first magnetization curve and the hysteresis loop of the cobalt ferrite sample. The saturation magnetization (270 kA/m) is lower than the literature data (398 kA/m, see Ref. [3]). A possible explanation for this difference is spin canting. In the 1980s it was observed that a reduction in particle size brings about a decrease in the saturation magnetization [6]: it was suggested that the surface layer contains spins that are not collinear with the magnetic field. They occupy a constant thickness independently of the particle size.

A different source of explanation comes from the fact that when magnetic oxides are produced through precipitation in basic medium, non-magnetic compounds are formed on the surface [7]. These compounds contain non-magnetic iron ions in hydrated form, mainly $(HFeO)^{-2}$, $Fe(OH)^{-4}$ and $FeO(OH)^{-2}$. With the purpose of quantifying this effect, Gribanov and coworkers [8] measured the saturation magnetization of the precipitates obtained from the coprecipitation of ferrous and ferric salts in alkaline medium. They observed an important effect of the base on the saturation magnetization of the solid phase, and as a consequence the magnetic properties are strongly affected by the synthesis process used.

From the experimental data of the saturation magnetization it is possible to estimate the amount of Co(II) per unit cell assuming an ideal cobalt ferrite structure with a lattice constant of 0.8359 nm and taking into account that each Co cation contributes 4 Bohr magnetons. Thus, we obtain that there are 4.6 Co per unit cell, i.e. 0.575 Co per subcell. On the other hand, atomic absorption data in our sample yield the empirical formula $CoFe_{5.32}O_{11.93}$ [9], from which we can estimate 0.34 cobalt atoms per subcell. This finding suggests the presence of other (more

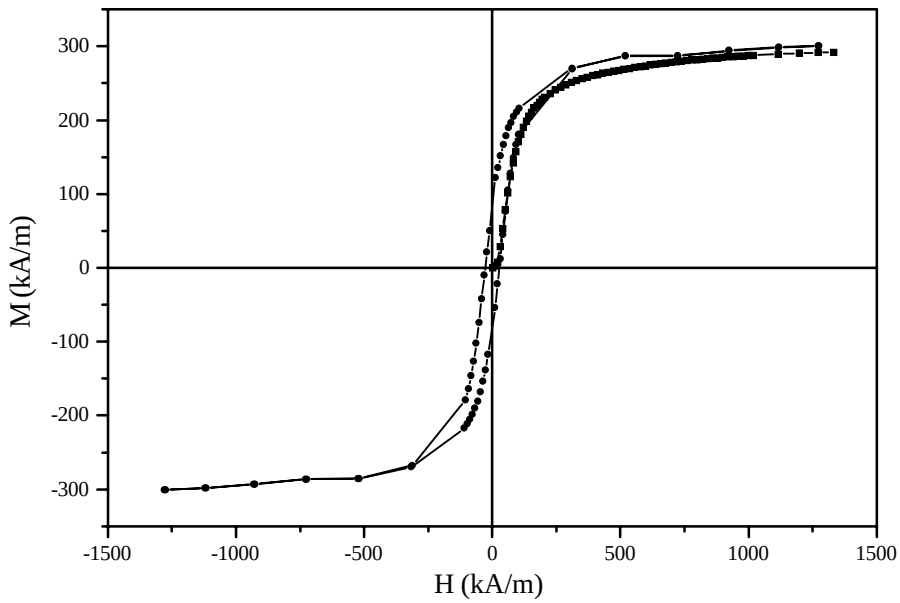

Fig. 2. Magnetization curve and hysteresis loop of cobalt ferrite powder measured with the magnetometer.

magnetic than Co-ferrite) phases, so that most likely our material is a mixed one, containing both magnetite and Co-ferrite.

From Fig. 2 we observe that the system can be considered as a hard magnetic material, due to its low initial permeability and relatively high coercive intrinsic field ($H_{c,i}$). It is important to remark that the initial permeability ($\mu_i = 1.94$) is very low in comparison to that of other soft ferrites as Mn–Zn ferrites ($\mu_i = 1000$) or Ni–Zn ferrites ($\mu_i = 650$). However, other aspects suggest a magnetically soft character: the remnant magnetization ($\mu_0 M_r = 0.103\,T$) is quite small as compared to that of hard magnetic materials: for instance, $\mu_0 M_r = 0.38\,T$ for barium or strontium ferrites. Also, the value of the saturation magnetic induction ($B_s = 0.339\,T$) is similar to other soft ferrites: for example (48% Mn, 52% Zn), OFe_2O_3 and (36% Ni, 64% Zn) OFe_2O_3, present $B_s = 0.36\,T$ and $B_s = 0.29\,T$, respectively. Finally, although $H_{c,i} = 27.5\,kA/m$ shows a hard character, this is not as pronounced as in granate structure ferrites, whose intrinsic coercive field is around $237\,kA/m$. We can note that the high value of $H_{c,i}$ could be due to structural defects as well as to the presence of cobalt in the ferrite [10]. Hence, the possibility of controlling the cobalt content in the ferrite may allow us to synthesize them with an intermediate behavior between soft (magnetite) and hard (ideal cobalt ferrite).

4.2. Differential permeability of suspensions

Fig. 3 shows the differential relative permeability, $\mu_{r,dif}$, of ferrite suspensions. Three curves are displayed in these graphs: line "1" corresponds to the first application of the magnetic field ramp; the line labeled "2" includes the data obtained by decreasing the field from its maximum value, and finally, curve "3" includes the data obtained by increasing the field again. As a general characteristic, we observe a decrease in the permeability with the internal magnetic field, which is explained by the magnetic saturation of the suspension. The maximum in the permeability for curve "1" manifests a hysteresis which in principle could be of magnetic origin, and that will be discussed below (Section 4.3).

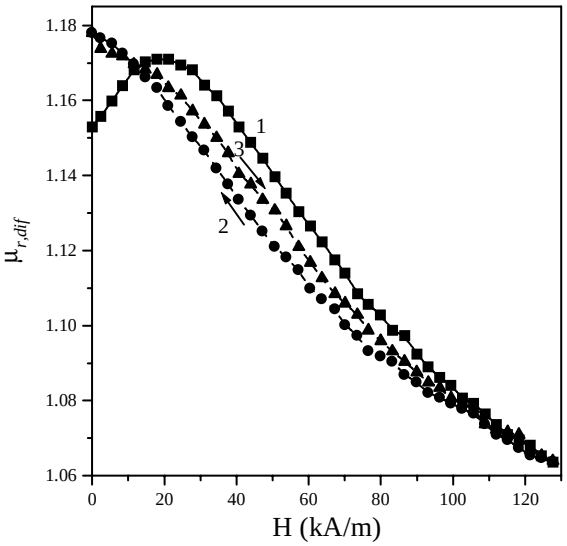

Fig. 3. Differential relative permeability of a cobalt ferrite suspension in silicone oil and Aerosil-300, as a function of the internal magnetic field ($\phi = 0.2$). Key: "1", first application of increasing magnetic field; "2", data for decreasing field from its maximum value; "3", second increasing field ramp.

It is important to remark that the data of the series "1" are unique, since the suspension should get structured during the first application of the field; the reason why curves "2" and "3" are below the first one must be magnetic hysteresis. Actually we expect this behavior in the presence of a remnant magnetization which will decrease the differential permeability for the second application. This remnant magnetization exists because the rotational Brownian time is large compared to the duration of the experiment. On the contrary, for suspensions of a material without magnetic hysteresis, as carbonyl iron, the differential permeability of iron suspensions changes with the field in an entirely different way as compared to ferrite suspensions (compare Fig. 4 with Fig. 3): the absence of hysteresis is associated to a decreasing-field permeability curve ("2" in Fig. 4) always above that corresponding to the first field ramp.

4.3. Influence of the microscopic structure of MRF in the shape of the differential permeability curves

As above mentioned, one possible explanation for the maximum in $\mu_{r,dif}$ for ferrite suspensions at

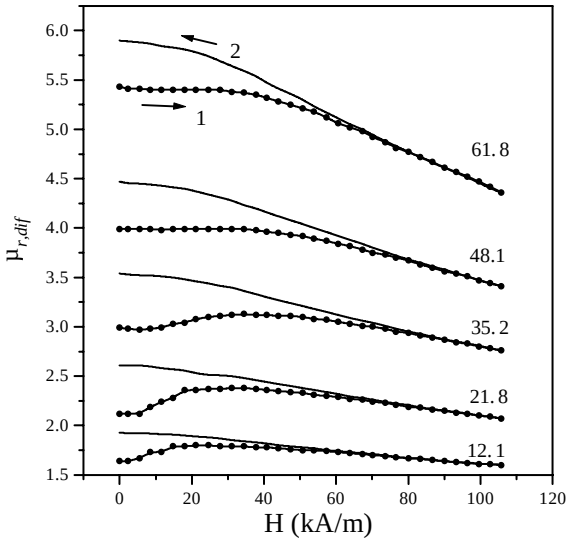

Fig. 4. Differential relative permeability as a function of the internal magnetic field in iron suspensions (liquids stabilized with silica gel) for different volume fractions (%). Curve labels as in Fig. 3.

low volume fraction (Fig. 3) could be related to the existence of magnetic hysteresis in the particles (Fig. 2). Nevertheless, Fig. 4 shows that similar maxima are observed in carbonyl iron suspensions, that do not display any hysteresis. An alternative explanation exists: the maxima in $\mu_{r,dif}$ can also be associated with the formation of microscopic structures due to particle–particle interactions when the field is first applied. In order to clarify that hypothesis, we performed permeability measurements in three kinds of carbonyl iron suspensions that we will call "liquids stabilized with silica gel", "non-structured solids" and finally "structured solids".

We call "liquids stabilized with silica gel" to colloidal suspensions of carbonyl iron in silicone oil adding silica gel in the amount mentioned above. In the preparation of "non-structured solids" we used: silicone oil, silicone elastomer and its catalyst. The amounts of oil, elastomer and catalyst were as follows: the volume of oil was $\frac{3}{4}$ the volume of elastomer; the mass of catalyst was 0.03 times the total mass of oil and elastomer. The "structured solids" were prepared in the same way as the non-structured ones, except that once the mixture is prepared it is placed during the curing process in a external magnetic field of 63 kA/m, in parallel direction to the cylinder axis.

Let us first consider the experimental results obtained for "liquids stabilized in silica gel" (Fig. 4). In this case the permeability decreases with the field as a consequence of the magnetic saturation; furthermore, we observe a maxima in permeability at low volume fractions. We can say that if particles are free to move by the action of the field, the maximum in $\mu_{r,dif}$ will be present, no matter if the particles display magnetic hysteresis or not.

In Fig. 5 we show the results obtained for "non-structured solids". Note first of all how the data corresponding to increasing and decreasing fields coincide at low volume fractions. This suggests that the lack of coincidence between curves of the type "1" (increasing field) and "2" (field decreasing from its maximum value) observed in Fig. 4 should be associated to the irreversible structuration during the first ramp in the system. If an elastomer matrix is used as in the systems of Fig. 5, the degrees of freedom of the particles must be greatly reduced, and the displacement of the particles inside the matrix should be hindered.

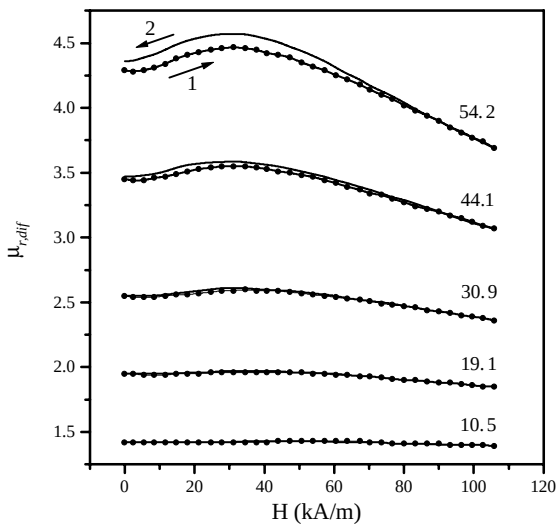

Fig. 5. Differential relative permeability as a function of the internal magnetic field in "non-structured solids" for different particle volume fractions (%). See Fig. 3 for curve labels.

Fig. 5 shows, however, that for high enough volume fractions the curves are again separated, and, furthermore, a maximum in permeability is also observed. Apparently, the elastomeric matrix cannot prevent the magnetic particles to move due to strong interactions, specially at the highest volume fractions. In order to further freeze the possible motions of the iron particles, we decided to prepare magnetic elastomers in a much more rigid epoxy matrix. We prepared a 50% particle volume fraction of carbonyl iron in Araldite 2019/AY103 with hardener Araldite 2019/HY991 (both from Ciba Polymeres, France), prepared according to the manufacturer's directions. In Fig. 6 we see that the maximum has disappeared and that the difference between permeabilities for increasing and decreasing field is much smaller. This reinforces the validity of our hypothesis of structuration during the measurement process as the reason for the maxima and the differences between trends of type "1" and "2". This is also observed in the results corresponding to "structured solids" (Fig. 7). The absence of maxima is understandable because the particles do not move during the measurement process, as they were previously aligned by the field applied before curing the suspension.

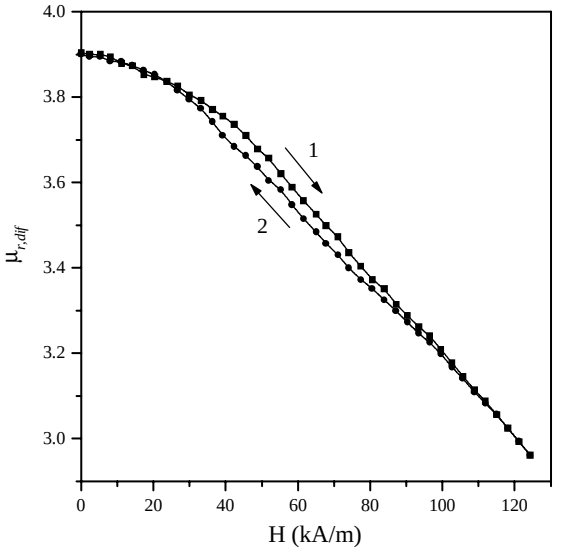

Fig. 6. Differential relative permeability as a function of the internal magnetic field in "non-structured solids" prepared in epoxy resin. Approximated particle volume fraction: $\phi = 0.5$. Curve labels as in Fig. 3.

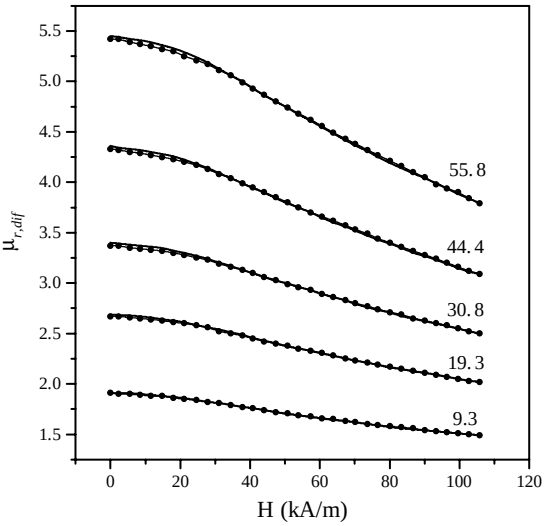

Fig. 7. Differential relative permeability as a function of the internal magnetic field in "structured solids" for different particle volume fractions (%). See Fig. 3 for curve labels.

4.4. Comparison with models

Besides the interpretation of the hysteresis (which is only noticeable at the highest volume fraction in elastomers) it is also interesting to use these experimental data to check the theories which aim to predict the magnetic permeability of a suspension. In the case where the particles are aligned by the field before curing a chain model is the simplest representation of the structure. Then, one can use a dipolar model to calculate the dipole of a chain but, if the particles have a high permeability, the enhancement of the field in the contact region can give rise to large changes in magnetization. In this case a finite element calculation using a permeability given by the Fröhlich Kennely law [1]: $M = \chi_i H/(1 + \chi_i/M_s H)$ allows to calculate the magnetic moment of a particle located inside an infinite chain. The parameters are the initial permeability: $\mu_i = 1 + \chi_i$ and the saturation magnetization, M_s: which is $M_s = 1360\,\mathrm{kA/m}$ for carbonyl iron. The volume

fraction is accounted for by the radius of the cylinder surrounding the two half spheres which constitute the unit cell of the simulation. We have compared in Fig. 8 the experimental curve at a volume fraction of 30.8% for a solid structured suspension (solid squares) to the predictions of different calculations. The three upper curves (E, D and C) correspond respectively to the initial permeabilities of 200, 132, 70. It is clear that both the shape and the magnitude differ strongly from the experimental data. It means that the particles are far from being arranged in ideal chains. We can suppose that there are many particles which are not in contact, since the viscosity of the polymer before curing is quite high and also the hydrodynamic resistance increase as the inverse of the gap between the particles. If we choose the lowest value for μ_i, then we can reproduce quite well the experimental behavior by taking a magnetic core of 98.5% instead of 100% (or in other words a gap of 0.03 between the particles). This couple of parameters actually fits as well all the other volume fractions. We see that these permeability measurements coupled with the calculation by FEM can give a quantitative measurement of the quality of the structuration inside the elastomer.

The unstructured elastomer has a lower permeability as we could expect. The comparison of the initial permeability for structured and unstructured elastomers are shown in Fig. 9 versus the volume fraction. The upper curve can easily be fitted by a straight line and the FEM model for infinite chains of spheres (curve D) also predicts a quasi-linear dependency. The curve C is the dipolar model for chains of dipoles [11]. The agreement is quite good, especially taking into account the absence of parameters (as the initial

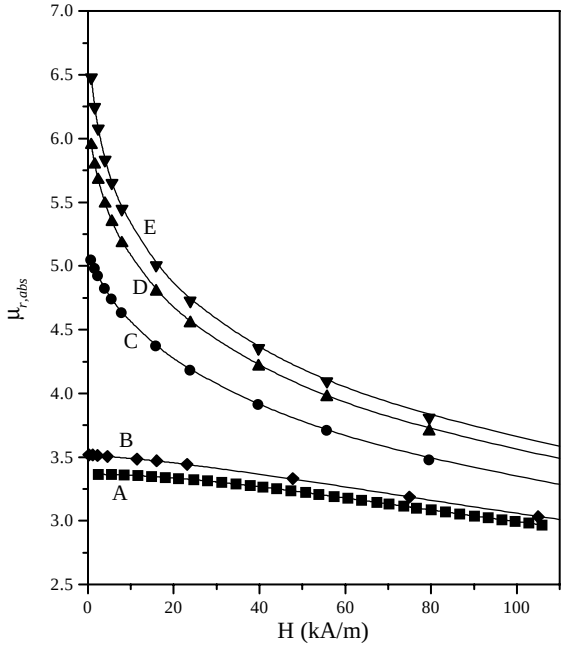

Fig. 8. Finite element method (FEM) calculations for structured solids at a particle volume fraction of 30.8%: (A) experimental absolute permeability, (B) FEM calculations with particle relative initial permeability $\mu_i = 70$ and magnetic core of 98.5% the total diameter, (C) FEM calculations with particle initial permeability $\mu_i = 70$, (D) same as C with $\mu_i = 132$ and (E) same as C with $\mu_i = 200$.

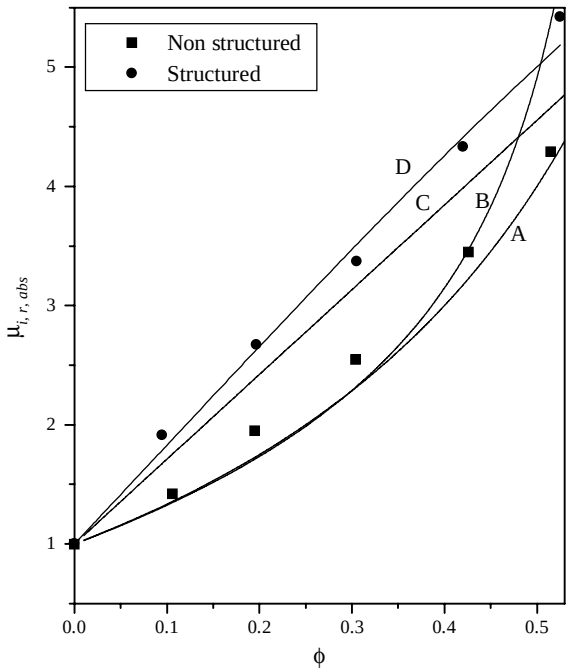

Fig. 9. Relative initial permeability of structured and non-structured iron elastomers as a function of volume fraction. (A) Mean field theory [12] with contrast factor $\beta \to 1$; (B) SC lattice [13]; (C) dipolar chain approximation [11]; (D) FEM calculation for chains with particle relative initial permeability $\mu_i = 70$ and magnetic core of 98.5% the total diameter.

permeability of the particles is large the result does not depend on its precise value). Concerning the unstructured elastomer, the curve A is the well known Maxwell–Garnett prediction [12] in the limit $\mu_p \gg 1$ and the curve B the prediction of a multipolar theory for simple cubic lattices [13]. The experimental results are almost linear in the volume fraction, whereas the models are clearly non-linear in the volume fractions. This discrepancy could be due to the fact that the particles are not well dispersed in the elastomers and still form loose aggregates.

5. Conclusion

We have measured the differential magnetic permeability of concentrated suspensions with the help of a simple method which can, as well, be used for a suspension flowing in a capillary. The results are given as a function of the field for different volume fractions of particles dispersed in a gel, in an elastomer and in a solid. The presence of a maximum in the differential permeability versus field curve is found when the particles have the possibility to move when the magnetic field is raised. This maximum disappears if the particles are fixed inside a hard polymer or if they are fixed inside linear aggregates formed by applying the field on the elastomer before curing. The comparison of the experimental results for structured elastomers with a FEM calculation on lines of spheres allow to conclude that the particles are not in contact. These measurements can be a way to check the quality of the structuration which is closely related to the performance of the magnetic elastomers [14,15].

Acknowledgements

Financial support through projects MAT98-0940 (CICYT, Spain) and INTAS99-0510 (EU) is gratefully acknowledged.

References

[1] D. Jiles, Introduction to Magnetism and Magnetic Materials, Chapman & Hall, London, 1991.
[2] J.R. Reitz, F.J. Milford, R.W. Christy, Fundamentos de la teoría electromagnética, Addison-Wesley Iberoamericana, Wilmington, 1996.
[3] P. Lethuillier, Magnétisme Pratique et Instrumentation, in: T. de Lacheisserie (Ed.), Magnétisme, Presses Universitaires de Grenoble, Grenoble, 1999.
[4] H. Tamura, E. Matijevic, J. Colloid Interface Sci. 90 (1982) 100.
[5] O. Volkova, Ph.D. Thesis, Université de Nice-Sophia Antipolis, 1998.
[6] K. Haneda, Can. J. Phys. 65 (1983) 1233.
[7] P. Belleville, J.P. Jolivet, E. Tronc, J. Livage, J. Colloid Interface Sci. 150 (1992) 453.
[8] N.M. Gribanov, E.E. Bibik, O.V. Buzunov, V.N. Naumov, J. Magn. Magn. Mater. 85 (1990) 7.
[9] J. de Vicente, A.V. Delgado, R.C. Plaza, J.D.G. Durán, F. González-Caballero, Langmuir 16 (2000) 7954.
[10] M. Ozaki, MRS Bull. Dec. (1989) 35.
[11] Y. Shkel, D.J. Klingenberg, J. Rheol. 43 (5) (1999) 1307.
[12] J.C. Maxwell-Garnett, Philos. Trans. Roy. Soc. London 203 (1904) 385;
J.C. Maxwell-Garnett, Philos. Trans. Roy. Soc. London 205 (1906) 237.
[13] M. Zuzovsky, H. Brenner, J. Appl. Math. Phys. 28 (6) (1977) 979.
[14] J.M. Ginder, M.E. Nichols, L.D. Elie, J.L. Tardiff, SPIE 3675 (1999) 131.
[15] G. Bossis, C. Abbo, S. Cutillas, S. Lacis, C. Métayer, Int. J. Mod. Phys. B 15 (2001) 564.